ISSN 1022-8594
JUJS

Vol. 43, No. 1, pp. 15-30

Convective Heat Transfer Analysis in a Trapezoidal Porous Cavity Using Al_2O_3-kerosene Nanofluid.

M. M. Billah[1, *], S. Yeasmin[1], M.M. Rahman[2] and Aminur Rahman Khan[3]

[1]*Department of Arts and Sciences, Ahsanullah University of Science and Technology, Dhaka-1208.*
[2]*Department of Mathematics, Bangladesh University of Engineering and Technology, Dhaka-1000.*
[3]*Department of Mathematics, Jahangirnagar University, Savar, Dhaka-1342.*

Abstract

A numerical study is conducted to investigate the transport mechanism of mixed convection in a lid-driven trapezoidal porous cavity filled with Al_2O_3-kerosene nanofluid. The left vertical wall moving at a constant speed and right inclined wall of the enclosure are insulated while the bottom horizontal wall is kept at constant temperature. The Galerkin weighted residual technique of finite element method (FEM) is used for simulation. Numerical solutions are obtained for a wide range of parameters. The streamlines, isotherm plots and the variation of the average Nusselt number at the bottom hot wall are presented and discussed elaborately. It is observed that the average heat transfer rate at the bottom surface is highest for the higher values of Darcy number.

Keyword: Nanofluid, heat transfer, porous medium, finite element method.

1. Introduction

With rapid number of growing industrial applications involving heat transfer such as in nuclear reactor, heat exchangers, air conditioning, solar collectors, electrical, micro electrical equipment etc. where heat is generated continuously during their respective processes it has been essential to release additional amount of heat to the surroundings quickly by means of heat transfer mechanism. For this purpose, Choi [1] first introduce nanofluid which is generally composed of a solid nanoparticles and a base fluid and has higher thermal conductivity compared to regular fluids. Another attractive method of heat transfer rate augmentation is using porous medium. In porous medium contact area increases between solid and liquid surface, as a result heat transfer rates ameliorates. Details

* Author for correspondence e-mail: mmb.as@aust.edu

for convection in porous media are represented in the book by Nield and Bejan [2]. Investigations are performed in convection heat transfer mechanism in great extent using both nanofluid and porous medium to optimize the heat removal process. Recent studies and applications about nanofluid flow and convection heat transmission in porous medium is reviewed by Khanafer and Vafai [3], Mahdi et al. [4], Kasaeian et al. [5].

In [6-8] convection heat transfer in presence of Lorentz force for complex shapes using Darcy model for porous media is illustrated with CVFEM simulation and the effects of nanofluid volume fraction, Hartmann number and Rayleigh number are presented. Sheikholeslami [9] performed a numerical study for CuO-H_2O forced convective nanofluid flow including uniform magnetic field in a porous cavity using mesoscopic method.

Mixed convection boundary layer flow over horizontal cylinder, vertical wedge are studied by Rashad et al. [10] and Gorla et al. [11] respectively. They represented the results in terms of velocity, temperature, and nanoparticles volume fraction, local nusselt number and Sherwood number. Cimpean and Pop [12] considered steady mixed convection flow through an inclined channel occupied with porous medium and presented analytical result for three different nanofluids where the authors considered parameters such as solid-volume fraction of nanoparticles, the mixed convection parameter, the inclination angle of the channel and the Peclet number. Recently, Aly et al. [13] investigated mixed convection considering a sloshing square non –Darcy porous cavity immersed in nanofluid with a baffle is inserted in the middle of the cavity by ISPH method. From the study they concluded that as the Darcy parameter decreases a higher resistance force for the fluid flow and a rise in the heat transfer rate occur. Very recently, Ahmed and Aly [14] analyzed mixed convection in a sloshing porous cavity heated by an inner rose considering Hazen-Dupain-Darcy model for porous medium. Tahmasbi et al. [15] simulated the effects of internal rotated heater and cooler with the various rotation directions and the optimized distribution of pore size in the porous media to maximize the mixed convection heat transfer rate using the pattern search optimization algorithm.

From the literature review, it is visible that few studies have been reported for steady mixed convective heat transfer of nanofluid saturated with porous medium. In this research, steady mixed convective flow in a trapezoidal shaped lid driven cavity saturated with porous medium is considered.

2. Mathematical Analysis

2.1 Physical Model

The physical model under current study with the system of coordinates is sketched in Fig. 1. The problem deals with a steady two dimensional flow of nanofluid confined in a lid-driven porous trapezoidal enclosure. The length of the bottom heated wall and height of the left vertical sliding wall of the enclosure are denoted by L and H, respectively. H to L ratio is taken as $\frac{1}{2}$. In addition, the left vertical sliding wall of the cavity is kept adiabatic and allowed to move from bottom to top at a constant speed V_0. Moreover, it is assumed that the temperature (T_h) of the bottom wall is higher than the temperature (T_c) of the top wall. The free space in the enclosure is filled with *Al_2O_3-kerosene* nanofluid.

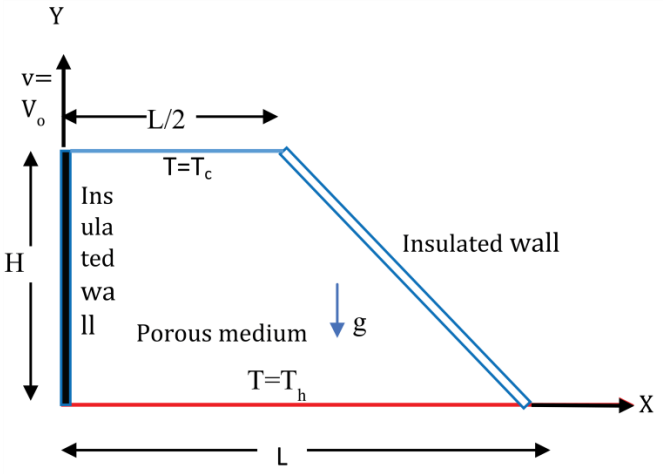

Figure 1. Schematic view of the physical model

2.2 Mathematical Model

The nanofluid in the enclosure is Newtonian, incompressible and laminar. The nanoparticles are assumed to have uniform shape and size. It is considered that thermal equilibrium exists between the base fluid and nanoparticles, and no slip occurs between the two media. The porous medium is considered isotropic, homogeneous and in thermal equilibrium with the fluid and Darcy-Brinkman-Forchheimer model is used for porous medium. The thermo-physical properties of the nanofluid are listed in Table 1. The physical properties of the nanofluid are considered to be constant except the density variation in the body force term of the momentum equation which is satisfied by the Boussinesq's approximation. Considering these premises stated above, the continuity, momentum and energy equations in two-dimensional form [16] can be written as:

$$\frac{\partial u}{\partial x}+\frac{\partial v}{\partial y}=0 \tag{1}$$

$$\frac{1}{\varepsilon^2}\left[u\frac{\partial u}{\partial x}+v\frac{\partial u}{\partial y}\right]=-\frac{1}{\rho_{nf}}\frac{\partial p}{\partial x}+\frac{\nu_{nf}}{\varepsilon}\left[\frac{\partial^2 u}{\partial x^2}+\frac{\partial^2 u}{\partial y^2}\right]-\frac{\nu_{nf}}{K}u-\frac{F_c}{\sqrt{K}}u\sqrt{u^2+v^2} \tag{2}$$

$$\frac{1}{\varepsilon^2}\left[u\frac{\partial v}{\partial x}+v\frac{\partial v}{\partial y}\right]=-\frac{1}{\rho_{nf}}\frac{\partial p}{\partial y}+\frac{\nu_{nf}}{\varepsilon}\left[\frac{\partial^2 v}{\partial x^2}+\frac{\partial^2 v}{\partial y^2}\right]-\frac{\nu_{nf}}{K}v-\frac{F_c}{\sqrt{K}}v\sqrt{u^2+v^2}+\frac{(\rho\beta)_{nf}}{\rho_{nf}}g(T-T_c) \tag{3}$$

$$u\frac{\partial T}{\partial x}+v\frac{\partial T}{\partial y}=\alpha_{nf}\left[\frac{\partial^2 T}{\partial x^2}+\frac{\partial^2 T}{\partial y^2}\right] \tag{4}$$

where u, v are the velocity along x, y coordinates respectively, p is the pressure, $\alpha_{nf}=\dfrac{\kappa_{nf}}{(\rho c_p)_{nf}}$ is known as the thermal diffusivity of nanofluids and other variables are defined in Nomenclature.

The consequent principles have been used to estimate the thermal and physical properties of nanofluids (more detailed in Tiwari and Das [17]), and Al-Weheibi et al. [18]):

The effective viscosity of nanofluids can be written as:

$$\mu_{nf} = \mu_{bf}(1-\phi)^{-2.5} \tag{5}$$

where ϕ is the nanoparticle volume fraction.

The effective density of nanofluid is expressed as

$$\rho_{nf} = (1-\phi)\rho_{bf} + \phi\rho_p \tag{6}$$

The heat capacitance of the nanofluids is given by

$$(\rho c_p)_{nf} = (1-\phi)(\rho c_p)_{bf} + \phi(\rho c_p)_p \tag{7}$$

The volumetric thermal expansion coefficient of nanofluids may be defined by

$$(\rho\beta)_{nf} = (1-\phi)(\rho\beta)_{bf} + \phi(\rho\beta)_p \tag{8}$$

The thermal conductivity model of solid-liquid mixture is the extension of Maxwell [19] experiment assuming the spherical shape of the nanoparticles which is obtained by Hamilton and Crosser [20] and is defined as follows:

$$\kappa_{nf} = \kappa_{bf}\frac{(n-1)\kappa_{bf} + \kappa_p - (n-1)\phi(\kappa_{bf} - \kappa_p)}{(n-1)\kappa_{bf} + \kappa_p + \phi(\kappa_{bf} - \kappa_p)} + \frac{(\rho c_p)_p \phi}{2}\sqrt{\frac{2\kappa_B T_C}{3\pi\mu_{nf} d_p}} \tag{9}$$

where d_p is the diameter of the nanoparticles and κ_B is the Boltzmann constant.

Forcheimer coefficients F_c is defined by Ergun's experimental investigation [21] as,

$$F_c = \frac{1.75}{\sqrt{150}\varepsilon^{3/2}} \tag{10}$$

Table 1. Thermophysical properties of different phases [22]

Property	**Fluid phase (Kerosene)**	**Solid phase (Al_2O_3)**
C_p (J Kg^{-1} K^{-1})	2010	765
ρ (Kg m^{-3})	810	3970
k (W m^{-1} K^{-1})	0.15	40
β (K^{-1})	$9{:}9 \times 10^{-4}$	0.89×10^{-5}
Pr	23.004	----

2.3 Dimensional Boundary Conditions

The suitable boundary conditions in dimensional form for the present model are as follows:

At the left walls: $u = 0, v = V_{o,}, \dfrac{\partial T}{\partial x} = 0$ (11a)

At the right inclined wall: $u = v = 0,\ \dfrac{\partial T}{\partial N} = 0$ (11b)

At the top wall: $u = v = 0, T = T_c$ (11c)

At the bottom wall: $u = v = 0, T = T_h$ (11d)

where *N* is the direction of normal to the inclined wall.

2.4 Non-dimensional form of Governing Equations

The non-dimensional forms of the governing equations (1)-(4) along with the boundary conditions (11a)-(11d) are attained by using the following non-dimensional variables:

$$X = \frac{x}{H},\ Y = \frac{y}{H}, U = \frac{u}{V_0},\ V = \frac{v}{V_0},\ P = \frac{p}{\rho_{nf}\, {V_0}^2},\ \theta = \frac{(T - T_c)}{\Delta T}, \Delta T = T_h - T_c \tag{12}$$

The resulting dimensionless equations are reduced to:

$$\frac{\partial U}{\partial X} + \frac{\partial V}{\partial Y} = 0 \tag{13}$$

$$\frac{1}{\varepsilon^2}\left[U\frac{\partial U}{\partial X} + V\frac{\partial U}{\partial Y}\right] = -\frac{\partial P}{\partial X} + \frac{1}{\varepsilon}\frac{\nu_{nf}}{\nu_f}\frac{1}{\mathrm{Re}}\left[\frac{\partial^2 U}{\partial X^2} + \frac{\partial^2 U}{\partial Y^2}\right] - \frac{\nu_{nf}}{\nu_f}\frac{1}{\mathrm{Re}\,Da}U - \frac{F_c}{\sqrt{Da}}U\sqrt{U^2 + V^2} \tag{14}$$

$$\frac{1}{\varepsilon^2}\left[U\frac{\partial V}{\partial X} + V\frac{\partial V}{\partial Y}\right] = -\frac{\partial P}{\partial Y} + \frac{1}{\varepsilon}\frac{\nu_{nf}}{\nu_f}\frac{1}{\mathrm{Re}}\left[\frac{\partial^2 V}{\partial X^2} + \frac{\partial^2 V}{\partial Y^2}\right] - \frac{\nu_{nf}}{\nu_f}\frac{1}{\mathrm{Re}\,Da}V - \frac{F_c}{\sqrt{Da}}V\sqrt{U^2 + V^2} + \frac{(\rho\beta)_{nf}}{\rho_{nf}\beta_f}Ri\theta \tag{15}$$

$$U\frac{\partial \theta}{\partial X} + V\frac{\partial \theta}{\partial Y} = \frac{\alpha_{nf}}{\alpha_f}\frac{1}{\mathrm{Pr}\,\mathrm{Re}}\left(\frac{\partial^2 \theta}{\partial X^2} + \frac{\partial^2 \theta}{\partial Y^2}\right) \tag{16}$$

Here the non-dimensional parameters Prandtl number (*Pr*), Grashof number (*Gr*), Reynolds number (*Re*), Richardson number (*Ri*) and Darcy number(*Da*) are defined respectively as,

$$Pr = \frac{\nu_{bf}}{\alpha_{bf}}, Gr = \frac{g\beta_{bf} H^3 (T_h - T_c)}{{\nu_{bf}}^2}, \text{Re} = \frac{V_o H}{\nu_{bf}}, Ri = \frac{Gr}{\text{Re}^2} \text{ and } Da = \frac{K}{H^2}$$

2.5 Non-dimensional Initial and Boundary Conditions

The non-dimensional form of the initial and boundary conditions are:

At the left walls: $U = 0, V = 1, \frac{\partial \theta}{\partial X} = 0$ (17a)

At the right inclined wall: $U = V = 0, \frac{\partial \theta}{\partial N} = 0$ (17b)

At the top wall: $U = V = 0, \theta = 0$ (17c)

At the bottom wall: $U = V = 0, \theta = 1$ (17d)

2.6 Calculation of Nusselt Number

The Nusselt number (Nu) is defined as the ratio of convective to conductive heat transfer across the boundary. The local Nusselt number can be defined as:

$$Nu_L = \frac{hL}{\kappa_{bf} \Delta T} \tag{18}$$

where κ_{bf} is the thermal conductivity of the base fluid and h is the convective heat transfer coefficient of the nanofluid flow and can be stated as:

$$h = -\kappa_{nf} \frac{\partial}{\partial y}(T - T_c) \tag{19}$$

Applying non-dimensional variables into Eq. (12), the heat transfer coefficient of the nanofluid can be written as:

$$h = -\frac{\kappa_{nf} \Delta T}{L} \frac{\partial \theta}{\partial Y} \tag{20}$$

Hence, the local Nusselt number for nanofluid can be stated as:

$$Nu_L = -\frac{\kappa_{nf}}{\kappa_{bf}} \frac{\partial \theta}{\partial Y} \tag{21}$$

The average Nusselt number at the bottom surface can be expressed as:

$$Nu_{av} = -\frac{\kappa_{nf}}{\kappa_{bf}}\int_0^1 \frac{\partial \theta}{\partial Y} dX \tag{22}$$

2.7 Stream Function

The relationships between stream function ψ and velocity components for two-dimensional flows are defined as:

$$U = \frac{\partial \psi}{\partial Y} \text{ and } V = -\frac{\partial \psi}{\partial X} \tag{23}$$

The positive sign of ψ denotes anti-clockwise circulation, and the negative sign indicated clockwise circulation.

3. Numerical Method

In this study, we use the Galerkin weighted residual technique of finite element method (FEM) as a numerical scheme. Billah et al.[23] and Zienkiewicz et al.[24] discussed this method elaborately. The finite element method begins by the partition of the continuum area of interest into a number of simply shaped regions known as elements. These elements may be different shapes and sizes. Within each element, the dependent variables are approximated using interpolation functions. In the present study erratic grid size system is considered especially near the walls to capture the rapid changes in the dependent variables. First we transformed the coupled governing equations (13)-(16) into sets of algebraic equations using finite element method to diminish the continuum domain into discrete triangular domains. Later on, we apply Newton–Raphson iteration technique to solve the set of the global nonlinear algebraic equations in matrix form through the partial differential equation solver with MATLAB interface. The solution procedure is repeated until the consequent convergence condition is satisfied: $\left|\Gamma^{m+1} - \Gamma^{m}\right| \le 10^{-7}$ where *m* is number of iteration and Γ is the general dependent variable.

3.1 Grid Refinement Check

A grid refinement test has been done for *Re*= 100, *Ri*= 1, $\varepsilon = 1$ *Da* = 10^{-2} and ϕ = 0.05 in a lid-driven trapezoidal porous enclosure. Five different non-uniform grid systems with the following number of elements within the resolution field: 1568, 2714, 3392, 4690 and 5243 are checked. The

numerical design is carried out for highly elements to develop an understanding of the grid fineness as presented in Fig. 2. The scale of Nu_{av} for 4690 elements shows a little difference with the results obtained for the other elements. Hence a grid size of 4690 elements is found to meet the requirements of the grid independency study.

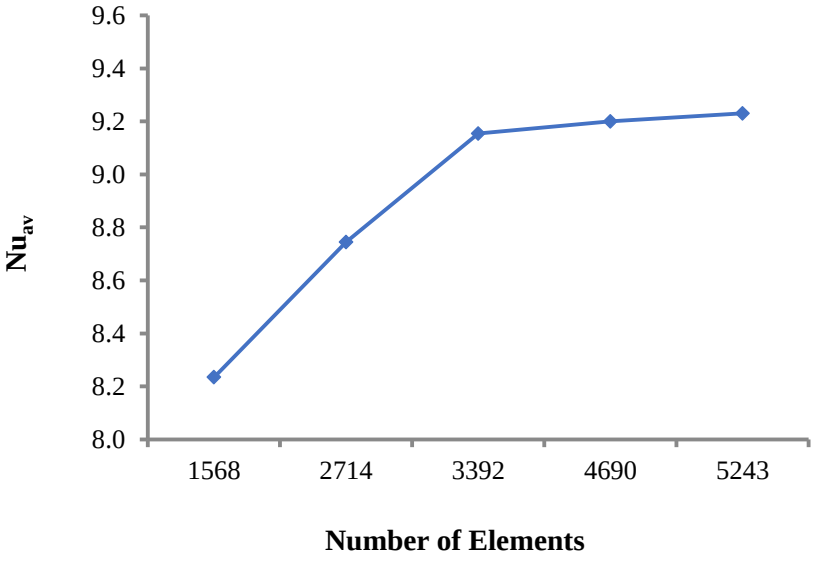

Figure 2. Grid independency study for Re = 100, Ri = 1.0, ε=1 Da = 10^{-2} and ϕ = 0.05

3.2 Code validation

The numerical code is validated against the problem of mixed convection in a lid-driven enclosure filled with nanofluids [25]. The cavity was cooled at the bottom wall and heated at the top wall while the rest of the walls were insulated. The comparison of the average Nusselt number between the result of the present code and the results found in the literature [25] for different solid volume fractions are tabulated in Table 2. The comparisons reveal an excellent agreement with the reported studies. This validation boosts the confidence in the numerical outcome of the present study.

Table 2. Comparison of *Nu* with those of Muthtamilselvan *et al*. [25]

ϕ	*Nu*		
	Ref [25]	Present study	% increase
0.0	2.26	2.38	5.51
0.02	2.40	2.56	6.71
0.04	2.56	2.75	7.50
0.06	2.73	2.94	7.81
0.08	2.91	3.14	7.90

4. Results and discussion

The present numerical study is carried out for Al_2O_3-kerosene nanofluids as working fluid with Prandtl number of Pr = 23.004. It is also assumed ε= 0.98 $d_p = 10$ nm, *Re*=100 $\phi = 0.05$. These considered values are selected to compute the value of some parameters which are not chosen arbitrarily. In this study, our attention is taken into account to explore the effects of governing parameters namely Darcy number (*Da*) and Richardson number (*Ri*). Here, the effect of Darcy number is investigated in the range of 10^{-5} – 10^{-2}. It is worth to note that the value of *Ri* is wide-ranging from 0.1 to 10 by varying Grashof number *Gr* to cover forced convection dominated region, pure mixed convection and free convection

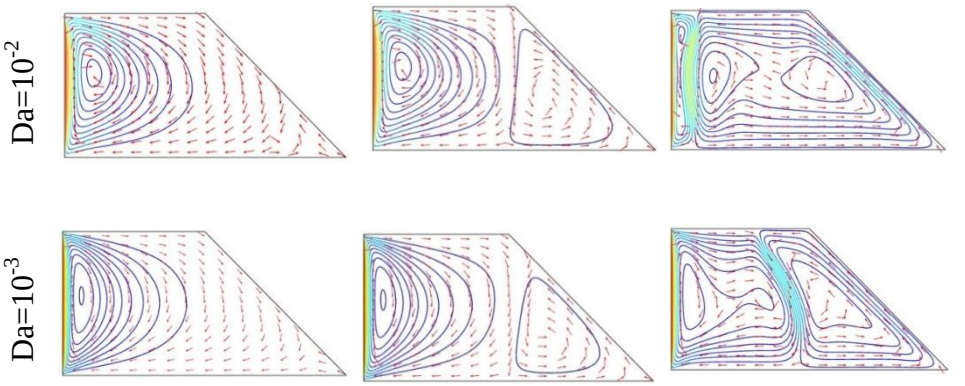

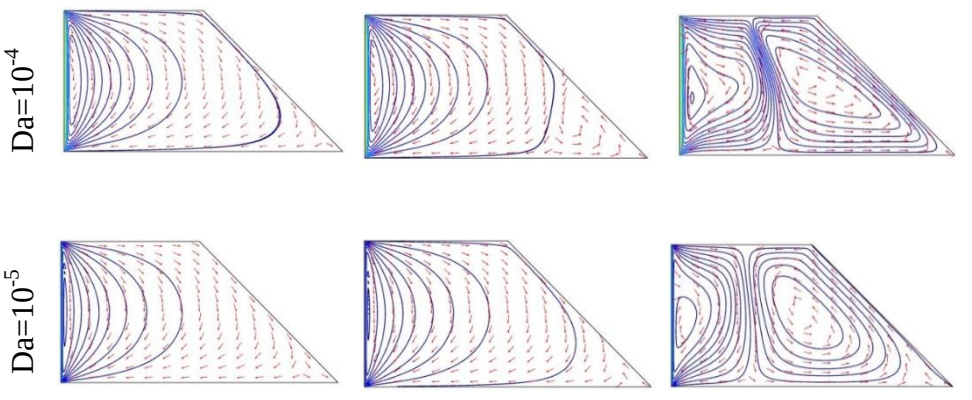

Figure 3. Effect of Da on streamlines for at (a) Ri = 0.1, (b) Ri= 1 , (c) Ri=10

dominated region. Moreover, the results of this study are presented in terms of streamlines and isotherms. Furthermore, the heat transfer effectiveness of the enclosure is displayed in terms of average Nusselt number *Nu*. As Darcy number Da is related to the cavity height H and the permeability K of the porous media, the study on the effect of this dimensionless number is comparable to the study of the effect of the permeability K.

The effect of various Darcy number on streamlines at Ri = 0.1, 1 and 10 is depicted in Fig. 3. At Ri=0.1 a major clockwise cell is generated by the lid dragging the neighboring fluid. As Da increases from 10^{-5} to10^{-2} gradually the clockwise vortex is increased at the left wall. The flow strength of the vortex is increased with the increasing values of Da. The major clockwise vortex near the left sliding wall is stronger at Ri=1 while it is compared with that of at Ri=0.1. As Da increases from 10^{-3} to 10^{-2} a secondary vortex is induced near the inclined wall and the strength of primary vortex is increased. At Ri=10, two strong vortices is formed one is clockwise and other one is anti-clockwise. As Da increases from 10^{-5} to 10^{-2} the strength of the vortex near the left wall is decreased and it gradually diminishes. On the other hand, the strength of the vortex near the inclined wall is increased and it start to occupy almost all area of the cavity. This is due to for porosity.

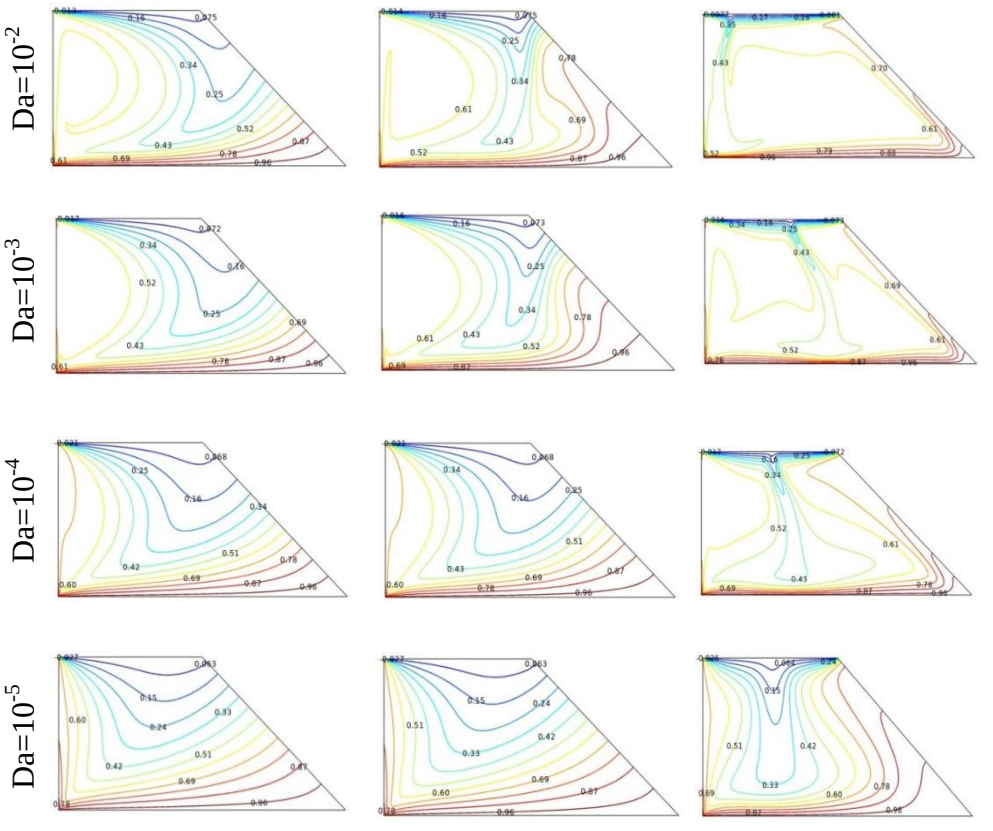

(a) Ri = 0.1 (b) Ri = 1 (c) Ri = 10

Figure 4. Effect of Da on Isotherms for at (a) Ri = 0.1, (b) Ri= 1 , (c) Ri=10 .

The influence of various Darcy number on isotherms at Ri = 0.1, 1 and 10 is shown in Fig. 4. From this figure it is observed that the isotherms are affected by the increase of porosity. It is noticed that the isothermal lines for higher values of Da are squeezed near the horizontal heated wall indicates strong convection. A high temperature levels and low temperature levels are also noticed near the heated wall and the cold wall respectively in narrow area.

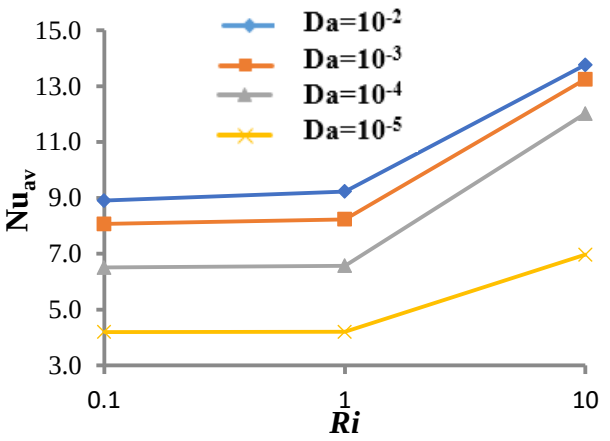

Figure 5. Effect of Darcy number on average Nusselt number at the heated surface in the cavity

The average Nusselt number (Nu_{av}) at the hot surface, which is a measure of the overall heat transfer rate as a function of Richardson number for the aforementioned values of the Darcy number (*Da)* is shown in Fig. 5. This figure shows a linear variation of the average Nusselt number with the Darcy number. As clearly be seen that the heat transfer increases with increasing Darcy number. It is noticed that the heat transfer rate increases very slowly up to the mixed convection region for all values of Da. But it upsurges very sharply from mixed convection region to free convection dominated region. For higher values of Da. However, the values of *Nu* are always maximum for the highest value of Da.

5. Conclusion

Mixed convection in a lid-driven trapezoidal porous enclosure filled with nanofluids is investigated numerically. Results for various parametric conditions are presented and discussed. From the above study, the following conclusions may be drawn:

- The inclusion of porous medium has produced an augmentation of the heat transfer coefficient.
- The Darcy number has more significant effect on the flow field than thermal field.

- The flow and thermal fields as well as the heat transfer rate inside the enclosure are strongly dependent on the Richardson number.
- The maximum heat transfer rate is found for higher values of Darcy number.

Nomenclature

c_p	Specific heat, $JKg^{-1}K^{-1}$
Da	Darcy number
d_p	Diameter of nanoparticle, m
F_c	Forchheimer coefficient
g	Acceleration due to gravity,
Gr	Grashof number
H	Height of the cavity, m
h	Heat transfer coefficient of
k	thermal conductivity, Wm^{-1} K^{-}
K	Permeability, m^2
L	Length of base wall, m
m	Mass, Kg
n	Empirical nanoparticle shape
Nu	Nusselt number
p	Dimensional modified
P	Dimensionless modified
Pr	Prandtl number
Re	Reynolds number
Ri	Richardson number
T	Fluid temperature, K
T_C	Cold temperature, K
T_h	high temperature, K
u,v	Dimensional nanofluid
U,V	Dimensionless nanofluid
V_o	Lid velocity along y direction,
x, y	Cartesian coordinates, m
X,Y	Dimensionless coordinates

Greek symbols

α	Thermal diffusivity, m^2s^{-1}
β	Thermal expansion
ϕ	Nanoparticles volume
ε	Porosity
Ψ	The sphericity of
ψ	Stream function
μ	Viscosity, Pa s
ν	Kinematic viscosity, m^2s^{-1}
κ	Thermal conductivity,
θ	Dimensionless temperature
ρ	Density, Kg m^{-3}

Subscript

av	Average
bf	Base fluid
p	Nanoparticles
nf	Nanofluid

References

[1] S.U.S. Choi. Developments and Applications of Non-Newtonian Flows, ASME, New York, 1995, FED- 231/MD- 66, pp. 99–105.

[2] D.A. Nield and A. Bejan. Convection in Porous Media, Springer, New York, 2013.

[3] K. Khanafer and K. Vafai. Applications of nanofluids in porous medium, Journal of Thermal Analysis and Calorimetry, 2019, 135, pp. 1479–1492.

[4] R.A. Mahdi, H.A. Mohammed and K.M. Munisamy and N.H. Saeid. Review of convection heat transfer and fluid flow in porous media with nanofluid, Renewable and Sustainable Energy Reviews, 2015, 41, pp. 715–734.

[5] A. Kasaeian, R.D. Azarian, O. Mahian, L. Kolsi, A.J. Chamkha, S. Wongwises and I. Pop. Nanofluid flow and heat transfer in a porous media: A review of the latest developments, International Journal of Heat and Mass Transfer, 2017, 107, pp. 778-791.

[6] M. Sheikholeslami, Z. Ziabakhsh and D.D. Ganji. Transport of Magnetohydrodynamic nanofluid in a porous media, Colloids and Surfaces A: Physicochemical and Engineering Aspects, 2017, 520, pp. 201-212.

[7] M. Sheikholeslami and S. A. Shehzad. CVFEM simulation for nanofluid migration in a porous medium using Darcy model, International Journal of Heat and Mass Transfer, 2018, 122, pp. 1264-1271.

[8] M. Sheikholeslami. Numerical approach for MHD Al_2O_3-water nanofluid transportation inside a permeable medium using innovative computer method, Computer Methods in Applied Mechanics and Engineering, 2019, 344, pp. 306-318.

[9] M. Sheikholeslami. Numerical investigation for CuO-H_2O nanofluid flow in a porous channel with magnetic field using mesoscopic method, Journal of Molecular Liquids, 2018, 249, pp. 739-746.

[10] A.M. Rashad, A.J. Chamkha and M. Modather. Mixed convection boundary-layer flow past a horizontal circular cylinder embedded in a porous medium filled with a nanofluid under convective boundary condition, Computers and Fluids, 2013, 86, pp. 380–388.

[11] R.S.R. Gorla, A.J. Chamkha and A. M. Rashad. Mixed convective boundary layer flow over a vertical wedge embedded in a porous medium saturated with a nanofluid: natural convection dominated regime, Nanoscale Research Letters, 2011, 207.

[12] D.S. Cimpean and I. Pop. Fully developed mixed convection flow of a nanofluid through an inclined channel filled with a porous medium, International Journal of Heat and Mass Transfer, 2012, 55, pp. 907–914.

[13] A. M. Aly, Z. A. S. Raizah and M. Sheikholeslami. Analysis of mixed convection in a sloshing porous cavity filled with a nanofluid using ISPH method, Journal of Thermal Analysis and Calorimetry, 2019, 139, pp. 1977–1991.

[14] S. E. Ahmed and A. M. Aly. Mixed convection in a nanofluid-filled sloshing porous cavity including inner heated rose, Journal of Thermal Analysis and Calorimetry, 2020, 143, pp. 275–291.

[15] M. Tahmasbi, M. Siavashi, H. R. Abbasi and M. Akhlaghi. Mixed convection enhancement by using optimized porous media and nanofluid in a cavity with two rotating cylinders, Journal of Thermal Analysis and Calorimetry, 2020, 141, pp. 1829–1846.

[16] M. Rajarathinam, N. Nithyadevia and A.J. Chamkha. Heat transfer enhancement of mixed convection in an inclined porous cavity using Cu-water nanofluid, Advanced Powder Technology, 2018, 29, pp. 590-605.

[17] R.K. Tiwari and M.K. Das. Heat transfer augmentation in a two-sided lid-driven differentially heated square cavity utilizing nanofluids, International Journal of Heat and Mass Transfer, 2007, 50, pp. 2002-2018.

[18] S.M. Al-Weheibi, M.M. Rahman, M.S. Alam and K. Vajravelu. Numerical simulation of natural convection heat transfer in a trapezoidal enclosure filled with nanoparticles, International Journal of Mechanical Sciences, 2017, 131-132, pp. 599-612.

[19] J.C. Maxwell. A Treatise on Electricity and Magnetism. Cambridge University Press, Cambridge, 2010, 2.

[20] R.L. Hamilton and O.K. Crosser. Thermal Conductivity of Heterogeneous Two-Component Systems. Industrial & Engineering Chemistry Fundamentals, 1962, 1, pp. 187-191.

[21] S. Ergun. Fluid flow through packed columns, Chemical Engineering Progress, 1952, 48, pp. 89–94.

[22] M. Mahmoodi and Sh. Kandelousi, Cooling process of liquid propellant rocket by means of kerosene-alumina nanofluid, Propulsion and Power Research, 2016, 5, pp. 279-286.

[23] M.M. Billah, M.M. Rahman, M. A Razzak, R. Saidur and S. Mekhilef. Unsteady buoyancy-driven heat transfer enhancement of nanofluids in an inclined triangular enclosure, International Communications in Heat and Mass Transfer, 2013, 49, pp. 115-127.

[24] O.C. Zienkiewicz, R.L. Taylor and P. Nithiarasu. The Finite Element Method for Fluid Dynamics, Butterworth-Heinemann, Oxford, 2014.

[25] M. Muthtamilselvan, P. Kandaswamy, J. Lee. Heat transfer enhancement of copper-water nanofluids in a lid-driven enclosure, Communications in Nonlinear Science and Numerical Simulation, 2010, 15, pp. 1501-1510.